

FAST METHOD TO PREDICT AN EARING PROFILE BASED ON LANKFORD COEFFICIENTS AND YIELD LOCUS

T. Lelotte¹, L. Duchêne², and A.M. Habraken¹

¹ Department of Mechanics of materials and Structures, University of Liège
Chemin des Chevreuils 1, 4000 Liège, Belgium
e-mail: Thomas.lelotte, anne.habraken@ulg.ac.be

² COBO Department, Royal Military Academy
Avenue de la Renaissance 30, 1000 Brussels, Belgium

Keywords: yield locus, Lankford, earing profile prediction.

Abstract. *This paper compares three methods to determine the earing profile that appears during the deep-drawing test of a circular steel sheet. Three steel grades will be studied. The first method is an experimental test made by a hydraulic press. The second one is a finite element method (FEM) deep-drawing simulation using a micro-macro texture based constitutive law. The last one directly determines the general aspect of the earing profile from the yield locus which is computed from the initial texture. The goal of this study is to validate the last approach. So, an earing profile prediction can quickly be obtained just from material's texture.*

1 INTRODUCTION

Appearance of an earing profile during the circular cup deep-drawing of a circular blank is due to the anisotropy of the metal sheet. FEM simulations of deep-drawing process can predict the earing profile but it takes a long computation time and a lot of memory storage.

This article presents a texture based method to calculate Lankford coefficients for different orientations from the rolling direction (RD) of the metal sheet. It is very fast and, knowing that the cup height variations at the end of the deep-drawing are linked to the variations of Lankford coefficients by Yoon's formula [1], the general aspect of the earing profile appearing during a deep-drawing can be predicted.

Three methods to determine the cup height of a drawn steel sheet will be studied.

- The first method is an experimental deep-drawing test on the steel sheet. The cup height is directly measured on the resulting cup. The experience is the reference of the study.
- A FEM simulation of the deep-drawing test is done using a texture based constitutive law without texture updating (Minty [2,3]) and a texture based constitutive law with texture updating (Evol [2,3]). These laws are implemented in the finite element code LAGAMINE developed at the M&S department. At the end of the deep-drawing simulation, the height of the cup for different angles from RD is provided.
- At the M&S department, a module was developed to compute some sections of the yield locus from the initial texture of the material. Each section is in the $\sigma_{11} - \sigma_{22}$ plane or in a plane parallel to it. On these curves, the points representing the tensile tests for any angle from RD can easily be identified. The normals of the yield locus at these points define the Lankford coefficients corresponding to these orientations from RD. These coefficients can be transformed into cup heights using Yoon's formula.

The latter approach is much faster than the two others and requires less memory storage. The resulting cup height is also less accurate than the one computed by other methods but it gives a good shape of the earing profile.

The goal of the present article is to describe the texture method (the third one) and validate it by comparison with results of the two other methods.

2 DESCRIPTION OF THE DIFFERENT APPROACHES

The IF steel sheet and the deep-drawing process presented in this section have previously been investigated by Li et al. [4]. Experimental measurements of the cup height are available and have been extracted from Li et al. These authors also gave us the parameters required to achieve the deep drawing simulations: characterisation of the IF steel (elastic and plastic parameters and texture measurement of the steel sheet), geometry of the process, friction behaviour...

The hardening behaviour is obtained through a tensile test along the rolling direction. The isotropic hardening law described by equation (1) is used.

$$\sigma = K \cdot (\varepsilon_0 + \varepsilon_{plastic})^n \quad (1)$$

The hardening parameters are fitted on the experimental tensile test. The values are

$$\begin{aligned} K &= 574 \text{ MPa} \\ \varepsilon_0 &= 0.00626 \\ n &= 0.326 \end{aligned} \quad (2)$$

Finally, the elastic parameters are:

$$\begin{aligned} E &= 210000 \text{ MPa} \\ \nu &= 0.3 \end{aligned} \quad (3)$$

In the article, the global X axis is along the initial position of the rolling direction of the steel sheet (RD), the global Y axis is along the transverse direction (TD) and the global Z axis is along the normal direction (ND). Stress tensors in global axes are noted $\underline{\sigma}^G$ and stress tensors in local axes (which are the axes where the material properties are defined) are noted $\underline{\sigma}^L$.

2.1 Experimental test

A hydraulic press has been used for the deep-drawing tests. The punch force is applied by a hydraulic jack. The blankholder force is also applied by hydraulic jacks acting on the corners of the blankholder. The blankholder maintains the steel sheet during the deep drawing process in order to avoid wrinkling. Without any blankholder or with a too low blankholder force, wrinkles would appear at the zone of the sheet near the edges. A too high blankholder force would lead to failure of the steel sheet during the deep-drawing process. The geometry of the tools and the blank is defined in figure 1. The blank is a disc cut out the rolled steel sheet.

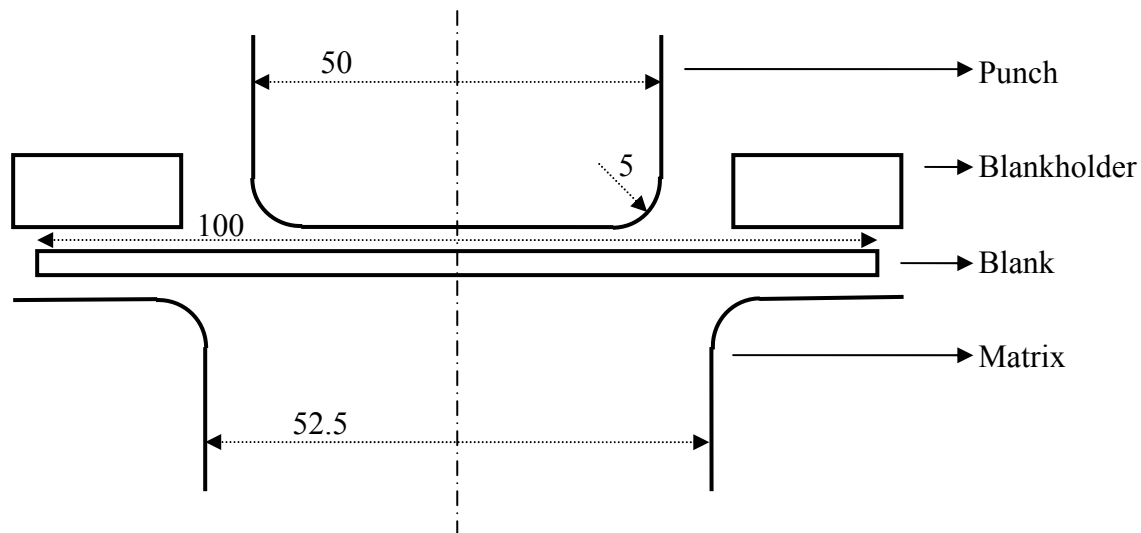


Figure 1: Geometry of the tools and the blank (dimensions in mm)

The anisotropy of the steel sheet can be taken into consideration by looking at the cup height of the deformed cup. The geometry of the blank and the tools is axisymmetric; with an isotropic steel sheet, the deformed cup would also be axisymmetric (no earing). The cup height corresponds to the height of the deformed cup which has been measured manually every 15° . Considering the orthotropic symmetry of the rolled steel sheet, the cup height measured from 0° to 90° should be symmetric (mirror-image) to this one measured from 90° to 180° . The same reasoning applies from 180° to 360° from RD. So the representation of the cup height in the range $[0^\circ, 90^\circ]$ is sufficient.

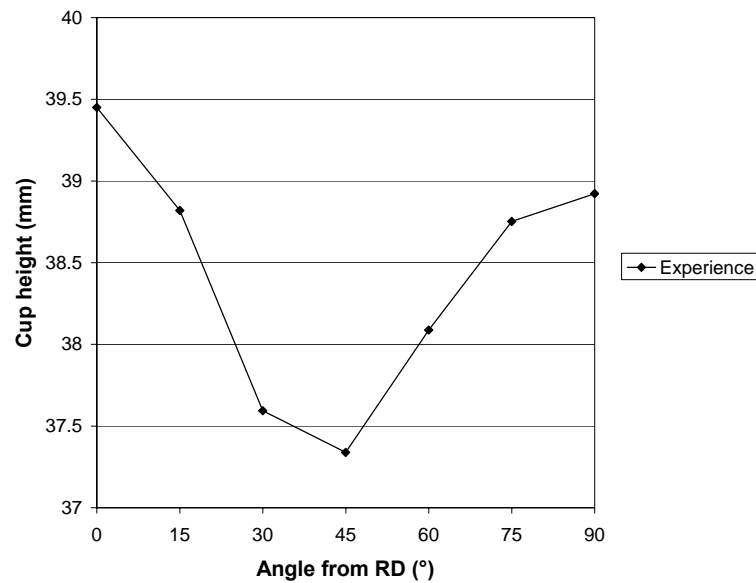


Figure 2 : Cup height for the experimental test

The complete deformed cup exhibits some minima at $45^\circ + k \cdot 90^\circ$ from RD and some maxima at $k \cdot 90^\circ$ from the RD. The maxima at 0° and 180° are greater than the maxima at 90° and 270° .

2.2 FEM simulation of the deep-drawing process

The geometry of the blank and the tools used for the FEM simulations of deep-drawing is the one from the experimental test. A 3D analysis, modeling only a quarter of the deep-drawing test, is achieved. Adequate boundary conditions must be imposed at the symmetry axes. These symmetry axes are defined as the global X and Y axes in the finite element mesh; the global Z axis is parallel to the punch displacement direction.

The tools are considered as perfectly rigid and are modeled by foundation elements. The tool mesh consists in triangular facets defined by 3 nodes. The volume of the tools is not modeled; only their external surface is meshed. In addition, for each tool, one pilot node is defined to determine the position of the tool during the deep-drawing simulation. Each pilot node fixes the position of the whole tool to which it is linked.

The blank is meshed with BLZ3D finite elements (see Zhu and Cescotto [5]). BLZ3D is a solid finite element with 8 nodes using a mixed formulation (in displacement, stress and strain). These elements are adapted for large strains and large displacements. One integration point per element is defined. As shown in figure 3, a quarter of the circular blank is meshed with one layer of 531 BLZ3D elements.

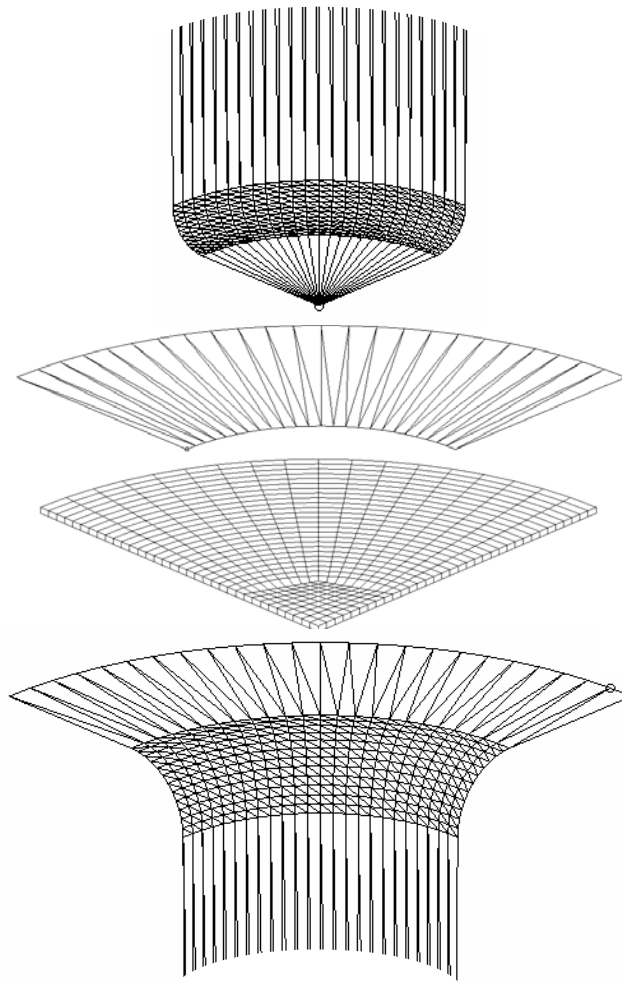


Figure 3 : Mesh of the blank and the three tools

At the beginning of the deep-drawing simulation, the pilot node of the blankholder is used to apply the blankholder force on the blank. Then, the pilot node of the punch drives the punch down to achieve the deep-drawing simulation. The pilot node of the matrix remains fixed throughout the process.

To represent correctly the anisotropy of the material behaviour, its texture is required. The FEM deep-drawing simulation of the blank is done using a micro-macro texture based constitutive law without texture updating called Minty [2,3]. The corresponding micro-macro texture based constitutive law with texture updating is Evol [2,3]. These laws are implemented in the finite element code LAGAMINE developed at the M&S department. From the experimental texture measurements, the ODFLAM procedure (recent version developed by the team of Professor Van Houtte) is used to compute a set of crystal orientations representative of the material behaviour. To reach a good compromise between accuracy and computation time, a set of 2000 crystals by integration point is used for these deep drawing simulations [3].

The first approach, without texture updating, is interesting because it is close to the texture approach presented in section 2.3. On the other hand, the approach with texture updating is closer to the experimental observations.

The cup height corresponds to the height of the deformed cup which has been computed from the nodal coordinates of the edge of the deformed cup (+/- every 5°). Considering the orthotropic symmetry of the rolled steel sheet, the cup height computed from 0° to 90° is symmetric (mirror-image) to this one computed from 90° to 180°.

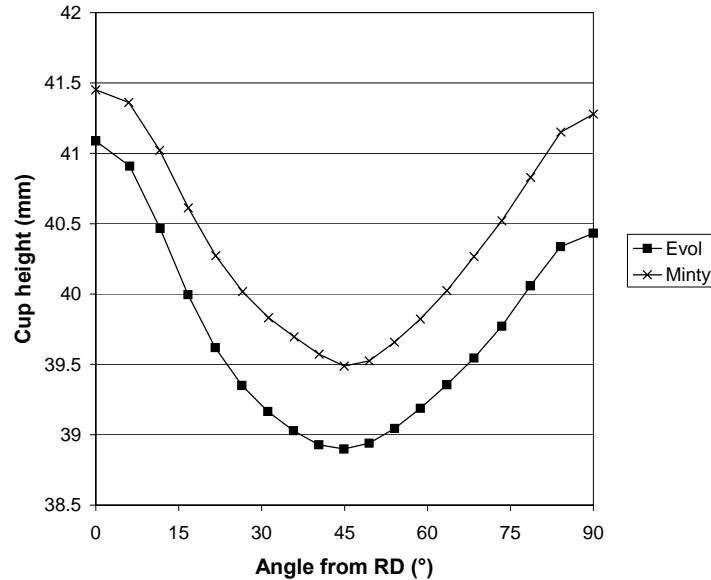


Figure 4 : Cup height for the FEM deep-drawing simulations

The two curves of deformed cup exhibit some minima at $45^\circ + k \cdot 90^\circ$ from RD and some maxima at $k \cdot 90^\circ$ from RD. The Minty curve is always upper than the Evol curve. The Evol curve presents a larger difference between the maxima at 0° and 180° and the maxima at 90° and 270° than the Minty curve.

2.3 Approach based on the yield locus

This approach is only based on the initial texture and the geometry of the blank and the tools. We have developed a program called “CPI” which computes the Lankford coefficients from the yield locus. The Lankford coefficients are linked to the normal of the yield locus. This program is based on a module developed by Laurent Duchêne to compute some π sections of the yield locus (sections made in the yield locus by a plane perpendicular to the hydrostatic stress direction).

The general principle is an exploration of the stress space with a fixed angular step. For each direction, the micro-macro law Minty [2,3] computes the yield stress. For a metal sheet, the important stress directions are the rolling direction RD (axis 1) and the transverse direction TD (axis 2), not the normal direction ND (axis 3). So the stress modes studied are some 2D stress modes in the RD-TD plane. Due to the volume conservation during plastic strains, the program works with deviatoric stress modes. $\hat{\sigma}_{13}$ and $\hat{\sigma}_{23}$ are fixed to zero and $\hat{\sigma}_{33}$ is fixed by the nullity of the trace.

The studied stress modes and the corresponding deviatoric part are presented in equation (4):

$$\underline{\hat{\sigma}}^G = \begin{pmatrix} a & c & 0 \\ c & b & 0 \\ 0 & 0 & -a-b \end{pmatrix} \quad \text{and} \quad \underline{\sigma}^G = \begin{pmatrix} 2a+b & c & 0 \\ c & a+2b & 0 \\ 0 & 0 & 0 \end{pmatrix} \quad (4)$$

The program computes the yield locus in the σ_{11} , σ_{22} , σ_{12} space. So there are only three parameters (a, b, c) which define each stress mode. As the deviatoric stress mode studied describes a direction in which the yield stress is computed (with Minty), it is normed.

$$\begin{aligned} a^2 + c^2 + c^2 + b^2 + (-a-b)^2 &= 1 \\ 2a^2 + 2b^2 + 2c^2 + 2ab &= 1 \end{aligned} \quad (5)$$

In equation (4), a pure tensile mode is characterized by a “c” value equal to 0.

If it is a pure shear mode, the “c” value is maximum (equation (6)) and the “a” and “b” values are equal to 0.

$$c_{\max} = \frac{\sqrt{2}}{2} \quad (6)$$

The range for “c” is $[0, \frac{\sqrt{2}}{2}]$ (negative “c” values are not taken into consideration). These values allow exploring all possible stress modes in the σ_{11} - σ_{22} - σ_{12} space (with $\sigma_{12} \geq 0$).

According to the amount of shear in the global axis (which fixes the “c” value) and the equation which norms the stress mode, it remains only one parameter to define. As it is shown on figure 5, for each chosen “c” value, a cone of stress mode directions is explored. The last parameter is the σ_{11}/σ_{22} ratio which links the “a” and the “b” values. It is defined with the angle α in equation (7).

$$b = a \tan \alpha \quad \text{with } \alpha \text{ ranging from } -90^\circ \text{ to } 90^\circ \quad (7)$$

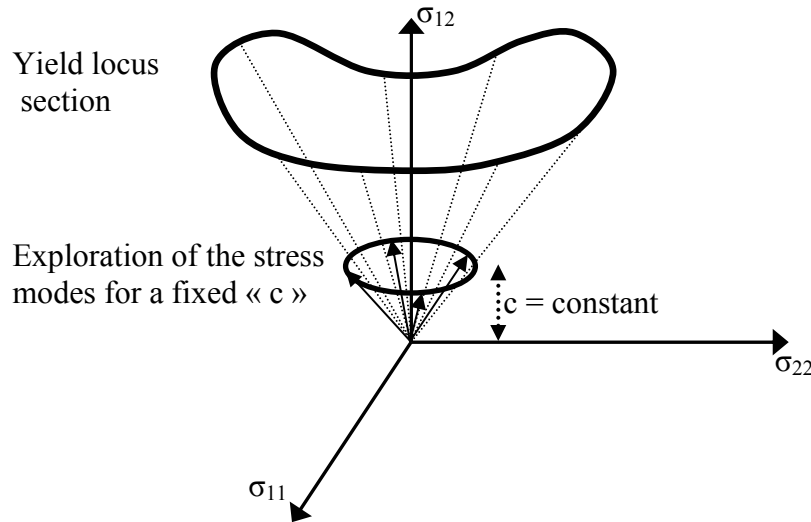


Figure 5 : Principle of the CPI program

The angular step for the variation of α is often taken equal to one degree and each value of α defines one explored stress mode. As the “c” value is fixed and the “b” value depends on

the “a” value (equation (7)), the equation which norms the stress mode (equation (5)) gives the “a” value in function of “c” and α .

$$a = \pm \sqrt{\frac{\frac{1}{2} - c^2}{1 + \operatorname{tg} \alpha + \operatorname{tg}^2 \alpha}} \quad (8)$$

So, the program computes a section of the yield locus for each “c” value chosen in the allowed range and for α evolving 0° to 360° .

Another application of CPI program is the exploration of particular stress modes. One stress mode corresponding to a pure tensile test in local axes (for example, a pure tensile test at an angle θ of 15° from RD) can be expressed in global axes as a stress mode containing some shear stress components.

If the local stress mode is given in function of the global stress mode:

$$\sigma^L = \begin{pmatrix} \sigma & 0 & 0 \\ 0 & 0 & 0 \\ 0 & 0 & 0 \end{pmatrix} = R \sigma^G R^T \text{ with } R = \begin{pmatrix} \cos \theta & -\sin \theta & 0 \\ \sin \theta & \cos \theta & 0 \\ 0 & 0 & 1 \end{pmatrix} \quad (10)$$

The pure tensile condition in local axes implies:

$$\text{Equation (1,2)} \Rightarrow a \cos \theta \sin \theta - b \cos \theta \sin \theta + c \cos^2 \theta - c \sin^2 \theta = 0 \quad (11)$$

$$\text{Equation (2,2)} \Rightarrow a + a \cos^2 \theta + b + b \cos^2 \theta + 2c \sin \theta \cos \theta = 0 \quad (12)$$

Note that “equation (i,j)” is the equation corresponding to the component (i,j) of the matrices of equation (10).

Equations (11) and (12) depend only on the “c” value and α because “a” and “b” depend on “c” and α . According to equations (7) and (8), a relation between the “c” value and α can be deduced for one chosen θ .

$$c = \sqrt{\frac{2}{5} + \frac{3(1 + \cos 2\alpha \cos 2\theta)}{10(-7 + 3 \cos 2\alpha \cos 2\theta - 5 \sin 2\alpha)}} \quad (13)$$

If the global stress mode is given in function of the local stress mode:

$$\sigma^G = R^T \sigma^L R \text{ with } R = \begin{pmatrix} \cos \theta & -\sin \theta & 0 \\ \sin \theta & \cos \theta & 0 \\ 0 & 0 & 1 \end{pmatrix} \quad (14)$$

Equation (14) is equivalent to equation (10) but each equation allows obtaining easily different relations.

$$\text{Equation (1,1)} \Rightarrow 2a + b = \sigma \cos^2 \theta \quad (15)$$

$$\text{Equation (2,2)} \Rightarrow a + 2b = \sigma \sin^2 \theta \quad (16)$$

A relation between α and θ is obtained by replacing “b” by a $\tan \alpha$ and dividing equation (16) by equation (15).

$$\alpha = \operatorname{arctg} \left(\frac{2 \operatorname{tg}^2 \theta - 1}{2 - \operatorname{tg}^2 \theta} \right) \quad (17)$$

Table 1 gives all the parameters corresponding to a chosen θ angle.

θ (°)	0	15	30	45	60	75	90
α (°)	-26.56	-23.95	-11.31	45.00	-78.69	-66.05	-63.70
c	0	0.306	0.530	0.612	0.530	0.306	0
a	0.82	0.73	0.51	0.20	-0.10	-0.33	-0.41
b	-0.41	-0.33	-0.10	0.20	0.51	0.73	0.82

Table 1 : Parameters in function of the angle θ from RD

The points of the yield locus corresponding to a pure tensile test at 0° and 90° from RD are on the section obtained with $c = 0$. The α value from equation (17) defines the exact position on that section. The same process gives the points corresponding to the other pure tensile tests.

Figure (6) presents the yield locus section of the IF steel for the “c” values in table 1. The points corresponding to pure tensile tests are highlighted.

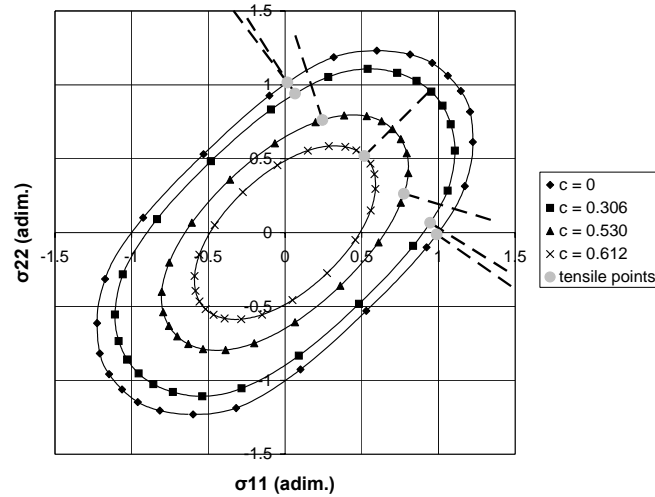


Figure 6 : Yield locus sections projected in the $\sigma_{11} - \sigma_{22}$ plane (scaled by the tensile yield stress along RD)

The normal to the yield locus at these points is linked to the value of the Lankford coefficient for all the chosen directions from RD. The angular step for α can be fixed and, in this case, it is equal to one degree.

To be validated, the results of the CPI program are compared to the Lankford coefficients calculated with FEM tensile tests. These FEM simulations are performed on a rectangular sample (X axis length = 32, Y axis length = 12, Z axis length = 1,6). There are 160 elements to mesh the sample (BLZ3D, 8 elements along X axis, 4 along Y axis, 5 along Z axis). The constitutive law used is the micro-macro texture based constitutive law without texture updating (Minty [2,3]). The tensile direction is the X axis and seven simulations are achieved on seven samples taken each 15° from 0° to 90° from RD.

For each test, the Lankford coefficient is computed by the formula

$$r = \frac{\varepsilon_y}{\varepsilon_z} \quad (18)$$

ε_y and ε_z are the plastic strains along y and z axes.

θ (°)	0	15	30	45	60	75	90
r (FEM)	2.55	2.41	2.25	1.85	1.98	2.33	2.60
r (CPI)	2.56	2.43	2.18	1.85	2.01	2.36	2.62

Table 2 : Lankford coefficient in function of the angle θ from RD

The 15° angular step for θ in table 1 is reduced to 1° in figure (7).

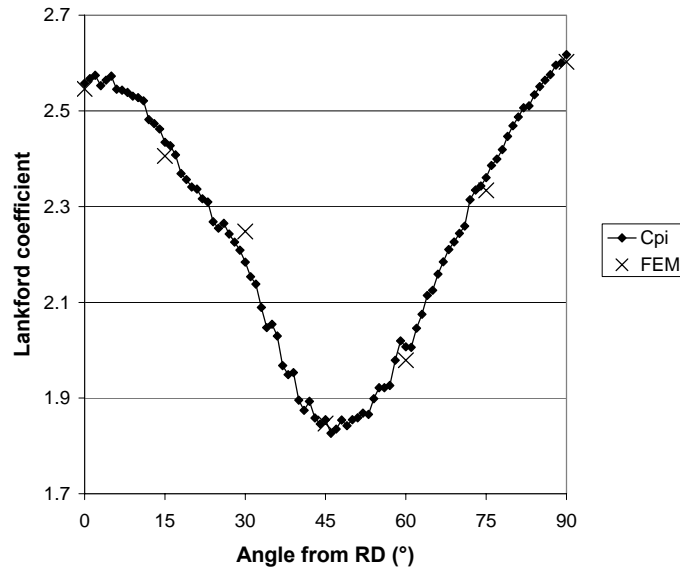


Figure 7 : Lankford coefficients computed by the CPI program and the FEM tensile tests

The two ways used to calculate the Lankford coefficients give very close results (figure 7 and table 2) but the CPI approach is quite faster (a few seconds for all the values) than the FEM approach (ten minutes by simulation with 2000 crystallographic orientations by integration point).

When the Lankford coefficients and the geometry of the blank and the tools are known, the cup height can be predicted using Yoon's formula (19), developed in [1].

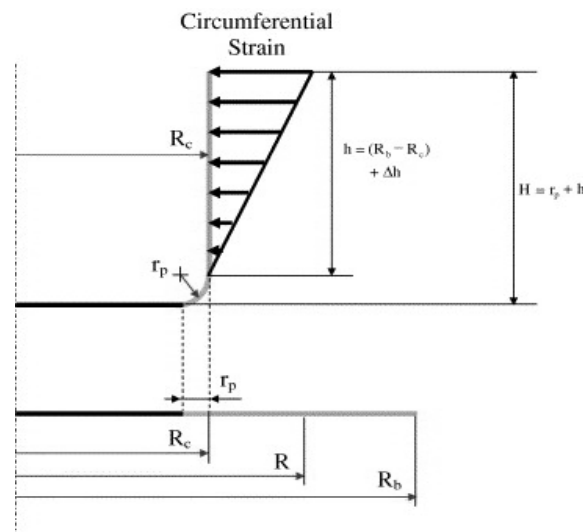


Figure 8 : Initial blank and drawn cup [1]

Only four geometrical parameters are relevant according to Yoon's hypotheses (see figure 8): the blank radius R_b , the punch profile radius r_p , the punch radius R_p and the matrix opening radius R_d . In the formula, it is assumed that the mid-plane of the drawn cup is located at the middle of punch and matrix opening radii (the thickness effect is neglected). So, R_c is taken equal to the average of R_p and R_d .

$$H_\theta = r_p + (R_b - R_c) + \frac{r_{\theta+90}}{(r_{\theta+90} + 1)} \left((R_c - R_b) + R_b \ln \left(\frac{R_b}{R_c} \right) \right) \text{ from [1]} \quad (19)$$

H_θ is the cup height calculated for an angle θ from RD. It depends on the Lankford coefficient calculated for an angle $\theta+90^\circ$ from RD. To calculate the cup height for an angle θ ranging from 0° to 90° , the Lankford coefficient must be known in the range $[90^\circ, 180^\circ]$. Considering the orthotropic symmetry of the rolled steel sheet, the Lankford coefficients measured from 0° to 90° should be symmetric (mirror-image) to those measured from 90° to 180° . If the Lankford coefficients are computed in the range $[0^\circ, 90^\circ]$, they are also known in the range $[90^\circ, 180^\circ]$.

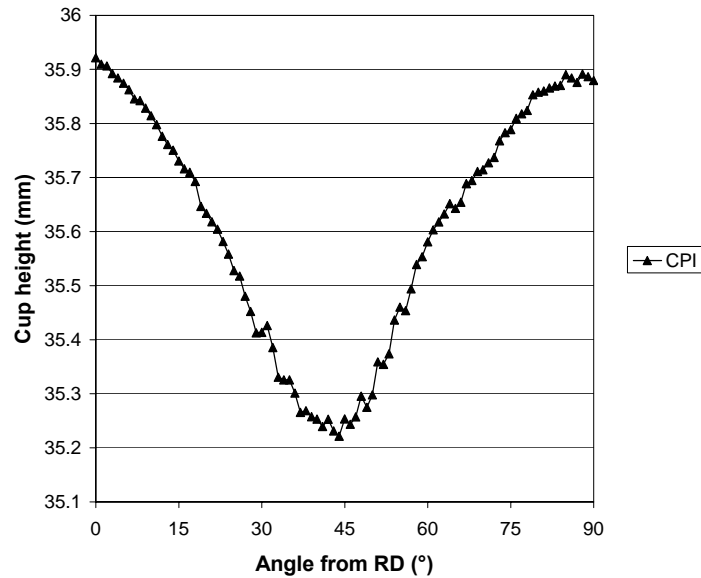


Figure 9 : Cup height for the CPI approach and Yoon's formula

The resulting complete deformed cup exhibits some minima at $45^\circ+k*90^\circ$ from RD and some maxima at $k*90^\circ$ from the RD. The maxima at 0° and 180° are very close to the maxima at 90° and 270° but a little bit larger.

3 COMPARISON AND DISCUSSION

The different approaches are compared in this section. It is important to note that the cup height depends on the lubrication technique used between the blank and the tools for the experimental test and on the corresponding friction coefficient fixed between the blank and the tools for the FEM simulation. The cup height calculated with Yoon's formula and the Lankford coefficients is an analytical approximation that does not depend at all on the lubrication. So, to allow a meaningful comparison of the different results, it is better not to take into account the importance of the lubrication and study the earing profile which is quite less sensitive to the friction behaviour.

The earing profile takes the minimum cup height as origin and represents the variations from this zero.

Figure 10 presents the earing profile obtained experimentally, with the two FEM constitutive laws and with the CPI program coupled with Yoon's formula.

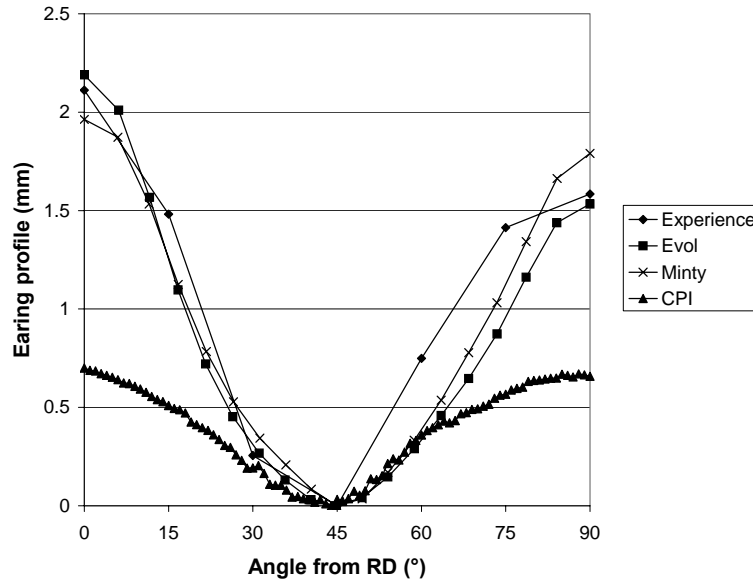


Figure 10 : Comparison of the earing profiles for the IF steel (experimental results from [4])

The FEM simulations of deep-drawing are close to the experimental test, especially when the texture is updated. The CPI program (with Yoon's formula) predicts 4 ears, in agreement with experience and FEM simulations, and the resulting earing profile exhibits the extrema on the good location. The general aspect of the curve is good too; the rate is greater on the left of the minimum than on the right but the difference between the maxima at 0° and 180° and the maxima at 90° and 270° is not as large in the CPI and Minty curves than in the experimental and Evol curves. This effect can be attributed to the texture evolution. Yoon's formula underestimates the size of the ears but the goal of this approach is a fast estimation of the general aspect of the earing profile.

4 OTHER MATERIALS

The earing profile prediction methods presented in this paper were also validated on two other deep-drawing processes with other materials. Another IF steel with four ears and one steel with six ears were analysed.

4.1 4 ears materials

The analysis presented in section 2 and 3 was performed on the IF steel studied in [6,7]. Figure 11 shows the earing profile obtained with the different approaches.

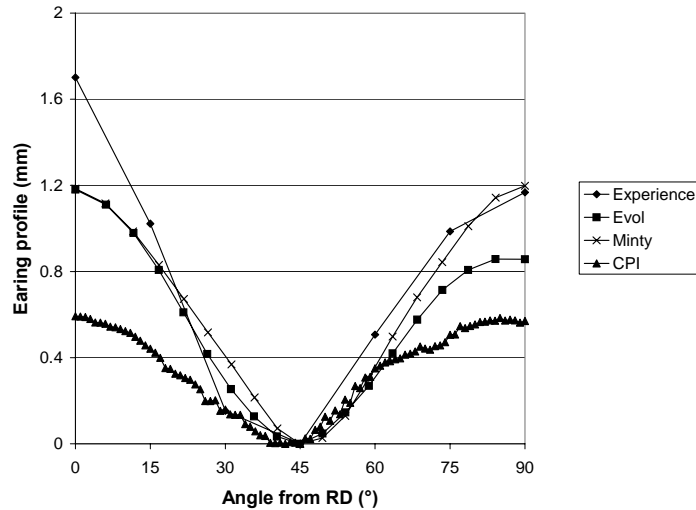


Figure 11 : Comparison of the earing profiles for the four ears steel (experimental results from [7])

The earing profile predicted by the CPI program is close to the profile predicted by the FEM deep-drawing simulation with the Minty constitutive law but with a smaller amplitude. The experimental test and the FEM simulation with the Evol constitutive law exhibit a larger difference between the maximum at 0° from RD and the maximum at 90° from RD. In this case, the texture evolution is taken into account. This time again, the general aspect predicted by the CPI program is good but the ears are underestimated.

4.2 6 ears material

To validate the CPI approach, the tests were also achieved on a third steel. The mechanic characteristics of this steel were provided by the Max Planck Institute of Dusseldorf. This material is interesting because it has a very anisotropic texture and its deep-drawing produces six ears.

Unfortunately, quantitative experimental deep-drawing results were not available. So the results of the CPI program were only compared to a FEM deep-drawing simulation with the Minty constitutive law.

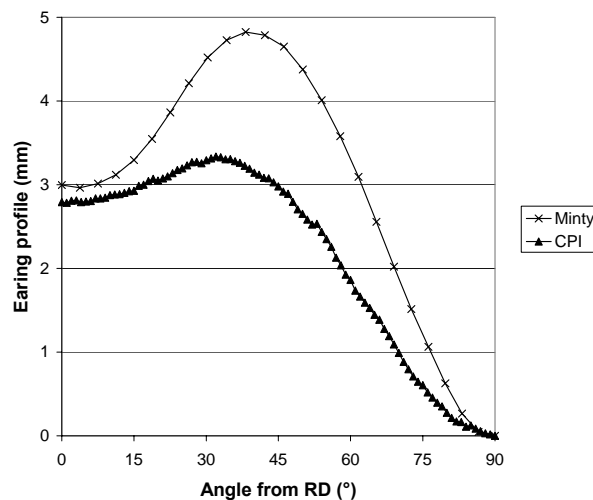


Figure 12 : Comparison of the earing profiles for the 6 ears steel

The FEM simulation exhibits one minimum at 4° from RD and one maximum at 38° from RD. The CPI program exhibits one minimum at 4° from RD too and one maximum at 31° from RD. These results are good and prove that the CPI approach works with a very anisotropic texture too.

5 CONCLUSIONS

The CPI program was developed to make possible a very fast prediction of the deep-drawing earing profile just from the initial texture and some geometrical features of the process. It was tested on three different materials. Each time, the results give a consistent general aspect of the earing profile of the drawn cup.

However, this approach always underestimates the height of the ears (it is an effect of Yoon's formula, already noted in [1]) and does not take into account some effects due to texture evolution (in particular, the gap between different maxima of the earing profile).

ACKNOWLEDGMENTS

A.M. Habraken is mandated by the National Fund for Scientific Research (Belgium). The authors thank the Belgian Federal Science Policy Office (Contract P5/08) for its financial support.

REFERENCES

- [1] J.W. Yoon, F. Barlat, R.E. Dick, M.E. Karabin, Prediction of six or eight ears in a drawn cup based on a new anisotropic yield function. *International Journal of Plasticity*, **22**, 174-193, 2006.
- [2] A.M. Habraken, L. Duchêne, Anisotropic elasto-plastic finite element analysis using a stress-strain interpolation method based on a polycrystalline model. *International Journal of Plasticity*, **20**, Issue 8-9, 1525-1560, 2004.
- [3] L. Duchêne, FEM study of metal sheets with a texture based, local description of the yield locus. Ph. D. Thesis, University of Liège, Belgium, 2003.
- [4] S. Li, E. Hoferlin, A. Van Bael, P. Van Houtte, Application of a texture-based plastic potential in earing prediction of an IF steel. *Advanced Engineering Materials*, **3**, No. 12, 990-994, 2001.
- [5] Y.Y. Zhu, S. Cescotto, Transient thermal and thermomechanical analysis by F.E.M. *Computers and Structures*, **53**, No. 2, 275-304, 1994.
- [6] L. Duchêne, P. de Montleau, F. El Houdaigui, S. Bouvier, A.M. Habraken, Analysis of texture evolution and hardening behavior during deep drawing with an improved mixed type FEM element. *Proceedings 6th International Conference : NUMISHEET*, 2005.
- [7] S. Li, E. Hoferlin, A. Van Bael, P. Van Houtte, C. Teodosiu, Finite element modeling of plastic anisotropy induced by texture and strain path change. *International Journal of Plasticity*, **19**, 647-674, 2003.